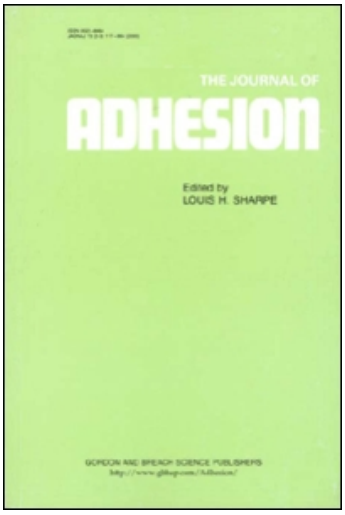

The Journal of Adhesion

Publication details, including instructions for authors and subscription information:
http://www.informaworld.com/smpp/title~content=t713453635

The Formation of Epoxy/Metal Interphases: Mechanisms and Their Role in Practical Adhesion

Jérôme Bouchet[a]; Alain-André Roche[a]
[a] Ingénierie des Matériaux Polyméres, Laboratoire des Matériaux Macromoléculaires, FRANCE

Online publication date: 08 September 2010

To cite this Article Bouchet, Jérôme and Roche, Alain-André(2002) 'The Formation of Epoxy/Metal Interphases: Mechanisms and Their Role in Practical Adhesion', The Journal of Adhesion, 78: 9, 799 — 830
To link to this Article: DOI: 10.1080/00218460213836
URL: http://dx.doi.org/10.1080/00218460213836

The Journal of Adhesion, 78: 799–830, 2002

0021-8464/02 $12.00 +.00
DOI:10.1080/00218460290010520

THE FORMATION OF EPOXY/METAL INTERPHASES: MECHANISMS AND THEIR ROLE IN PRACTICAL ADHESION

Jérôme Bouchet
Alain-André Roche
Ingénierie des Matériaux Polyméres/Laboratoire des Matériaux Macromoléculaires, FRANCE

When epoxy/diamine systems are applied onto metallic substrates and cured, an interphase, having chemical, physical, and mechanical properties quite different from bulk polymer is created between the substrate and the polymer. The aim of this work is to understand the interphase formation mechanisms and their role in practical adhesion. Mechanisms were deduced from comparison of behaviors when either epoxy and diamine monomers or epoxydiamine monomer mixtures were applied onto aluminum, titanium, and gold-coated surfaces. Using various analytical techniques (DSC, FTIR, FTIR-RAS, ICP, and POM) we will show both a chemical sorption of the diamine monomers and a partial dissolution of the surface oxide and/or hydroxide metallic layer. Then, metallic ions diffuse through the liquid monomer layer and react with amine groups to form an organo-metallic complex by coordination bonding. When the complex concentration is higher than its solubility limit, these complexes may partially precipitate to form needle-sharp crystals. The liquid part of the organo-metallic complex forms, with the epoxy prepolymer, a new amorphous network having a lower glass transition temperature. This new biphase material can also contain complex crystals which act as short fibers, randomly dispersed in the polymer matrix or oriented in the vicinity of the polymer/metal interface, inducing an increase of the Young's modulus and a decrease of the elongation at break. By using a three-point flexure test, we have determined the effect of the interphase formation on the practical adhesion before and after hydrothermal aging. Results obtained point out that the epoxy/metal interphase significantly affects the initial practical adhesion. However, formation of organo-metallic complexes greatly improve practical adhesion after aging. The created complexes act as corrosion inhibitors.

Received 16 June 2001; in final form 25 April 2002.

Presented at the 24th Annual Meeting of The Adhesion Society, Inc., held in Williamsburg, Virginia, USA, 25–28 February 2001.

Address correspondence to A.-A. Roche, Ingénierie des Matériaux Polyméres, Laboratoire Macromoléculaires, INSA de Lyon, 20 Avenue Albert Einstein, F-69621 Villeurbanne Cedex, France. E-mail: alain-andre.roche@insa-lyon.fr

Keywords: Metal-diamine chemical reactions; Epoxy/metal interphase; Practical adhesion

INTRODUCTION

Knowledge and consideration of the interphase are important for both fundamental and practical adhesion aspects. Indeed, the interphase and its properties determine the final overall properties of composite systems (practical adhesion, corrosion resistance, and durability) made of two components; the substrate and the polymer. Epoxy-diamine mixtures are extensively used as adhesives or paints in many industrial applications. When they are applied onto metallic substrates and cured, epoxy-amine liquid monomers react with the metallic oxide and/or hydroxide to form chemical bonds [1, 2] increasing practical adhesion (or adherence) between the epoxy polymer and the substrate surface [3, 4]. Different studies report the influence of the nature of the metallic substrate on the cross-linking of the prepolymer [5]. Some authors have shown a catalytic effect of the substrate on the cross-linking mechanisms and the prepolymer adsorption onto metallic surfaces [6]. Others have attempted to determine the existence of specific monomer/substrate reactions. As an example, Dillingham and Boerio [7] have studied the polymerization of a diglycidyl ether of bisphenol A (DGEBA) and a triethylene tetramine (DGEBA-TETA) system applied onto aluminum by using both FTIR and XPS. Close to the polymer/metal interface, the hardener is partially protonated by aluminum hydroxides. Moreover, the polymerization is catalyzed by the presence of acidic hydroxyl groups, leading to the formation of an interphase. Nigro and Ishida [8] have studied an epoxy/BF3-monoethylamine system applied onto polished steel using FTIR. The epoxy conversion rate was more important in the polymer/metal interfacial region, suggesting the existence of chemical reactions with the steel surface. The epoxy prepolymer was applied onto the steel surface (without hardener) and the same phenomenon was still observed, suggesting that the chemical species formed at the steel surface were able to catalyze the homopolymerization of the epoxy monomer. Gaillard and coworkers [9–10] have shown that the DGEBA-DDA polymerization rate was faster on the zinc surface of galvanized or electrogalvanized steel than on polished steel. They concluded that the zinc metallic ions had a catalytic effect, leading to a higher extent of cross-linking. Some researchers have studied the adsorption of various monomers used as adhesives at the substrate surface [11–13]. Using FTIR, Kollek [14]

studied the polymerization of a diglycidyl ether of bisphenol A and a dicyandiamide (DGEBA-DDA) system applied onto aluminum and observed that both the DDA and the DGEBA monomers were adsorbed onto the aluminum oxide surface. For the DDA monomer, the adsorption was due to the acidic proton of the aluminum oxide. For the epoxy monomer, the adsorption was achieved by the oxirane (or epoxy) ring opening. Unfortunately, only a few papers [15–18] have dealt with molecular structures formed within the interphase region. Moreover, when epoxy resins are applied onto metallic substrates and cured, intrinsic and thermal residual stresses develop within the entire organic layer [19]. Intrinsic stresses are produced as a result of the mismatch between the active sites of the metallic substrate and the organic network and/or the formation of the polymer network. Thermal stresses are mostly developed during cooling [20] and are the result of thermal expansion mismatch between the metallic substrate and the polymer, or cure-induced shrinkage of the organic layer [21]. Whatever their source, these residual stresses reduce the practical adhesion and may induce cracks in coating materials [22–24], resulting in a drop of the overall performance of adhesives or paints. To gain a better understanding of epoxy/metal adhesion requires a full knowledge of chemical and physical reactions that take place within the epoxy/metal interphase [25, 26]. Thus, the polymer/substrate interphase is a complex region containing gradients of residual stresses and Young's modulus [27] resulting from structural rearrangement, intermolecular and interatomic interactions, and diffusion phenomena [25]. When the adhesion of epoxy/metal systems failed, it was possible not only to correlate the residual stresses at the interphase/metal interface with practical adhesion but also to correlate the theoretical adhesion and durability with the presence or not of some chemical species [28].

OVERVIEW OF THE PRESENT WORK

The aim of this paper was to understand the interphase formation when liquid epoxy-amine systems were applied onto several metallic substrates and to determine the role of that interphase in practical adhesion before and after hydrothermal aging.

The interphase region being the region where chemical, physical, and mechanical properties are different from those of the bulk polymer, we have compared chemical (a/e), physical (Tg), and mechanical (E) properties of the organic bulk material with organic coatings as a function of the coating thickness (from 30 μm to 1 mm [29]. Using a simple mixing law, it was possible to plot the variation of the various

measured parameters (Tg, a/e). These variations pointed out the interphase formation between the substrate and the part of the coating having bulk properties. To understand the chemical mechanisms leading to the interphase formation we applied, and left for three hours, either liquid epoxy or liquid amine monomers onto the metallic surface. The "modified" monomers were removed from the metallic surfaces and analyzed using various analytical tools to determine chemical reactions that may occur. Lastly, mixing the modified diamine monomer with the pure epoxy monomer allows us to obtain new materials having the same properties as the thinnest coatings.

EXPERIMENTAL

Materials

Substrates

Metallic substrates used in this study were 0.516 ± 0.005 mm thick commercial-rolled aluminum alloy (5754 from Péchiney, Voreppe, France) and 0.600 ± 0.005 mm thick commercial titanium alloy (Ti6Al4V from Aérospatiale, Suresnes, France). Titanium and aluminum sheets were made into squares of dimensions $100 \times 100\,mm^2$. For practical adhesion measurement, metallic substrates were prepared by die-cutting to provide identically sized strips ($50 \times 10\,mm^2$). Before any polymer application, aluminum and titanium substrate surfaces were ultrasonically degreased in acetone for 10 min and wiped dry with a soft absorbent paper. However, some aluminium and titanium panels were also degreased and chemically etched. Aluminium samples were immersed in a solution of 250 g/l of sulfuric acid, 50 g/l chromic acid, and 87 g/l aluminium sulphate octadecahydrate at 60°C for 20 min, rinsed in running tap water for 1 min, immersed in deionized water for 5 min, and wiped dry with a soft absorbent paper. Titanium samples were submerged in a solution of 10 g ammonium bifluoride, distilled water to 1 l, at room temperature for 2 min; rinsed in running tap water for 1 min, allowed to stand in deionized water for 5 min, and wiped dry with a soft absorbent paper. After surface treatment, all substrates were kept in an air-conditioned room (22 ± 2°C and $55 \pm 5\%$ R.H.) for 2 h. Some aluminium and titanium sheets were coated with gold (≈ 100 nm) using a SCD005 Sputter Coater from Bal-Tec.

Monomers and Polymers

The bifunctional epoxy prepolymer used was a liquid diglycidyl ether of bisphenol A (DGEBA, M = 348 g/mole, DER 332 from Dow

Chemical). The diamine curing agent used was either isophorone-diamine (IPDA or 3-aminomethyl-3,5,5-trimethylcyclohexylamine from Fluka) or the poly(oxypropylene diamine) (D400 from Huntsman, Everberg, Holland). Epoxy prepolymers and curing agents were used without further purification. Assuming a functionality of 4 for diamines and 2 for the epoxy monomer, a stoichiometric ratio (a/e = aminohydrogen/epoxy) equal to 1 was used throughout the work (except as otherwise mentioned). Homogeneous mixtures of DGEBA and diamine were achieved by stirring under vacuum (1 Pa) at room temperature for 1 h (Rotavapor RE211 from Büchi, Switzerland) to avoid air bubble formation. The epoxy-amine adhesive cure cycle [30–32] was adapted to obtain both the maximum of the cure conversion, (i.e., the highest glass transition temperature) and the entire interphase formation.

For IPDA, the curing cycle was: 3 h at 20°C, 20 → 60°C (2°C/min), 2 h at 60°C, 60 → 140°C (2°C/min), 1 h at 140°C, 140 → 190°C (2°C/min), 6 h at 190°C, cooling (8 h) in the oven to 20°C. For D400, the curing cycle was: 3 h at 20°C, 20 → 60°C (2°C/min), 2 h at 60°C, 60 → 100°C (2°C/min), 3 h at 100°C, cooling (8 h) in the oven to 20°C.

Diamine Analysis

To determine the chemical and physical changes that may appear in liquid monomers (IPDA or D400), they were applied between two degreased metallic substrates ($100 \times 50\,mm^2$) to form a 110–150 μm thick liquid layer and kept at room temperature for 3 h in a desiccator under continuous nitrogen flow to prevent any monomer carbonation or oxidation. The monomers were then scraped from the metallic surfaces with a PTFE spatula and stored in polyethylene vials under a nitrogen atmosphere. They are called "modified" monomers in the following work.

Experimental Techniques

Differential Scanning Calorimetry (DSC)

Differential scanning calorimetry (DSC) experiments were carried out in a Mettler DSC 30 apparatus to control the full polymerization of the organic layer and to determine the glass transition temperature (Tg) of either epoxy bulk materials (pure and "modified") or coatings of various thickness (from 30 to 1000 μm). Sealed aluminum pans containing 15–20 mg epoxy materials were heated from −50°C to 250°C at a rate of 10°C/min under a continuous flow of U-grade argon. Pieces of bulk and debonded organic coatings were weighed using a Mettler balance having a 1 μg sensitivity. The calorimeter was calibrated

with both indium and zinc. The glass transition temperature was determined by the onset point with a 1°C sensitivity for each coating of various thickness and also for the bulk material. To evaluate the Tg variation versus the coating thickness, we calculated the $(Tg)_{eq}$ value at thickness i using a mixing law:

$$(Tg)_{eq} = \frac{h_i Tg_i - h_{i-1} Tg_{i-1}}{h_i - h_{i-1}}.$$

The Tg_i value corresponds to the glass transition temperature of an h_i thick coating, and the Tg_{i-1} value corresponds to the glass transition temperature of an h_{i-1} thick coating. Plotting $(Tg)_{eq}$ versus the coating thickness corresponds to determining Tg profile versus thickness.

Inductively Coupled Plasma (ICP) Spectroscopy

To check for any metallic ion diffusion through the liquid diamine monomer after application onto a metallic surface, ICP spectroscopy was used. An ICP spectrometer (Modula by Spectro Analytical Instruments, Kleve, Germany) was used with a 2.5 kW plasma generator at 27 MHz and with UV (0.75 m, 2400 grooves mm^{-1}; 160–480 nm) monochromator, UV (0.75 m, 3600 grooves mm^{-1}) polychromator, and visible (0.75 m, 1200 grooves mm^{-1}) polychromator. A cross-flow nebulize was used to introduce the liquid sample. Deionized water was used as solvent.

Polarized Optical Microscopy (POM)

Visually, when liquid monomers were applied onto metallic substrates and left for 3 (IPDA) or 24 h (D400) on those metallic surfaces, and then were removed and poured into test tubes, a milky precipitate was visible. Drops of "modified" diamine precipitate were confined between two glass plates. Elsewhere, "modified" diamine precipitate was mixed with pure epoxy monomer (a/e = 1), and one drop of the mixture was mounted on a hot plate under a POM apparatus (Laborlux 12POLS from Leica, Wetzlar, Germany equipped with a hot plate FP82 from Mettler, Viroflay, France and a CCD-IRIS color video camera from Sony, Japan). Samples were heated from 30°C to 190°C at 10°C/min.

Fourier Transform Near-Infrared (FTNIR) Spectroscopy

To point out any new chemical bonding in "modified" monomers, a Fourier transform infrared spectrometer (FTIR; Magma-IR 550 from Nicolet) was used with Omnic FTIR software. The infrared spectra were recorded either in the 400–4000 cm^{-1} or in the 4000–7000 cm^{-1}

range using either a DTGS or a MCT/A detector. Transmission was used for both bulk and organic coatings after debonding from the metallic substrate. For each spectrum, 64 scans were collected at $4\,cm^{-1}$ resolution. The conversion rates of epoxy and amine groups were calculated by using the $4530\,cm^{-1}$ epoxy combination band and the $6500\,cm^{-1}$ amine band respectively. The $4623\,cm^{-1}$ aromatic C-H ring stretch combination band was considered as a reference. Thus, amine (X_a) and epoxy (X_e) conversion rates were determined using the ratio of the respective band areas (A) by

$$X_a = 1 - \frac{(A_{6500}/A_{4623})_t}{(A_{6500}/A_{4623})_{t=0}}$$

and

$$X_e = 1 - \frac{(A_{4530}/A_{4623})_t}{(A_{4530}/A_{4623})_{t=0}} \tag{2}$$

Once again, to evaluate the X_a and X_e variation versus the coating thickness we calculated the $(X_a)_{eq}$ and $(X_e)_{eq}$ values at thickness i using

$$(X_{a,e})_{eq} = \frac{h_i(X_{a,e})_i - h_{i-1}(X_{a,e})_{i-1}}{h_i - h_{i-1}}. \tag{3}$$

The $(X_{a,e})_i$ value corresponds to the amine or the epoxy conversion of an h_i thick coating and $(X_{a,e})_{i-1}$ value corresponds to the amine or the epoxy conversion of an h_{i-1} thick coating. Plotting $(X_{a,e})_{eq}$ versus the coating thickness corresponds to determining the $X_{a,e}$ profile versus thickness. We have determined and already reported the variation of the $(X_a)_{eq}/(X_e)_{eq}$ ratio as a function of the stoichiometric ratio (a/e) for such DGEBA/IPDA systems [33]. Using this calibration curve, it is possible to determine the variation of the (a/e) ratio versus the coating thickness. Moreover, for some systems homopolymerization phenomena were also studied as a function of the stoichiometric ratio, by using the ratio of the ether/phenyl band areas (A_{1120}/A_{830}).

Reflectance Infrared Spectroscopy

To determine the hydroxide layer dissolution when liquid monomers were applied onto the metallic surfaces, an infrared spectrometer (FTIR Magna-IR 550 from Thermo Optek, Montigny, France) was used with Omnic FTIR software. An Ever-Glo™ source was used along with a KBr beam splitter and DTGS-KBr detector. The midinfrared

spectra were recorded in the $400-4000\,cm^{-1}$ range. For each spectrum, 32 scans were collected at $4\,cm^{-1}$ resolution. A VeeMax^{TM} (from Spectra-Tech, Inc., Shelton, USA) variable angle specular reflectance/accessory was used at 80°.

Tensile Test

A tensile machine (2/M from MTS systems, Iury/Seine, France) fitted with a 10 kN full-scale load with a sensitivity of ± 0.1 N and a stiffness of 2.10^8 N/m was used to determine the Young's modulus of both modified bulk polymers and bulk polymer. Tests were performed at 10 mm/min.

Young's Modulus of Thin Films

This work was performed with a three-point flexure machine (FLEX3, Techmétal, Maizières-les-Metz, France) [34–35]. The crosshead displacement speed was 0.1 mm/min. A 50 N full-scale load cell with a sensitivity of ± 5 mN and a stiffness of 2.2×10^5 N/m was fitted under the crosshead. The load (P) versus displacement (δ) curves (P/δ curves) were recorded by the microcomputer and displayed on the PC screen in real time. The slopes of the P/δ curves within the linear region were then computed using a linear regression program. Experimental curve slopes were corrected to take into account the load cell stiffness as described previously [34]. For various spans (L_j), the apparent modulus $(E_{app})_j$ can be calculated from the slope (P/δ) of the load-displacement curve. According to Rippling et al. [36], the extrapolated Young's moduli of the substrate and the entire coated system can be obtained from curves of E_{app} as a function of h/L_j. It has been reported that the extrapolated Young's modulus is independent of the ratio b/h and, thus, the transverse effect (Poisson's ratio) will not be considered [35].

Practical Adhesion Measurement

This test was performed with a flexure machine (FLEX3, Techmétal, Maizières-les-Metz, France) fitted with a 1000 N full-scale load cell with a sensitivity of ± 0.1 N and a stiffness of 1.1×10^7 N/m, according to the ISO 14679-1997 standard, at a crosshead displacement speed of 0.5 mm/min. The DGEBA-IPDA mixture was applied onto degreased or chemically etched aluminium substrate by applying an exact amount of $0.5\,cm^3$ with a syringe on each sample. The adhesive-forming mould was made of RTV-501 (Rhone Poulenc). The adhesive block formed had dimensions $25 \times 5 \times 4$ mm^3 [37]. Either the ultimate load (F_{max}) or the ultimate displacement (d_{max}) was used to evaluate the practical adhesion of DGEBA-IPDA polymer on the metallic substrates. Hydro-

thermal aging (immersion in DI water at 40°C for 24 h) was used for some samples. Six samples were prepared and tested for each series.

Radius of Curvature Determination

The determination of the radius of curvature of coated substrates was carried out to point out the role of the interphase and, more particularly, the role of the organo-metallic complexes in the residual stresses developed in such sytems. Experiments were carried out with a flexure machine (FLEX3, Techmétal, Maizières-les-Metz, France) equipped with a 50 N full-scale load cell with a sensitivity of ± 5 mN and a stiffness of 2.2×10^5 N/m. Coated samples were placed on a planar and rigid material [29]. Assuming that the radius of curvature is large compared with both the length and the thickness of the multilayer beam ($R \gg L \gg h$), it can be considered that the length of the neutral axis is equal to its span. For such a curved multilayer beam of neutral axis length (L in mm) and maximal deflection (δ_{max} in mm) at the midspan ($L/2$), the radius of curvature (R_1 in mm) is given by

$$R_1 = \frac{L^2}{8\delta_{max}}$$

with

$$L \gg 2\delta_{max}. \quad (4)$$

RESULTS AND DISCUSSION

Interphase Characterization

According to curing cycles mentioned previously, the maximum glass transition temperatures of DGEBA-IPDA and DGEBA-D400 bulk polymer were, respectively, 163°C and 34°C. These values are in good agreement with previous work [31, 38]. Variation in the equivalent glass transition temperature as a function of the thickness of both DGEBA-IPDA and DGEBA-D400 coatings applied onto degreased titanium or gold-coated panels is shown in Figure 1. Regardless of coating thickness, for coatings applied on gold-coated substrates the equivalent glass transition temperatures were equal to the bulk ones, irrespective of the nature of the diamine. For the thinnest coatings on titanium ($< 50\,\mu$m), the equivalent glass transition temperature values were quite different from the bulk ones, irrespective of the nature of the diamine. For coating thicknesses between $50 < h < 600\,\mu$m, a gradient region was observed. When the coating thicknesses were greater

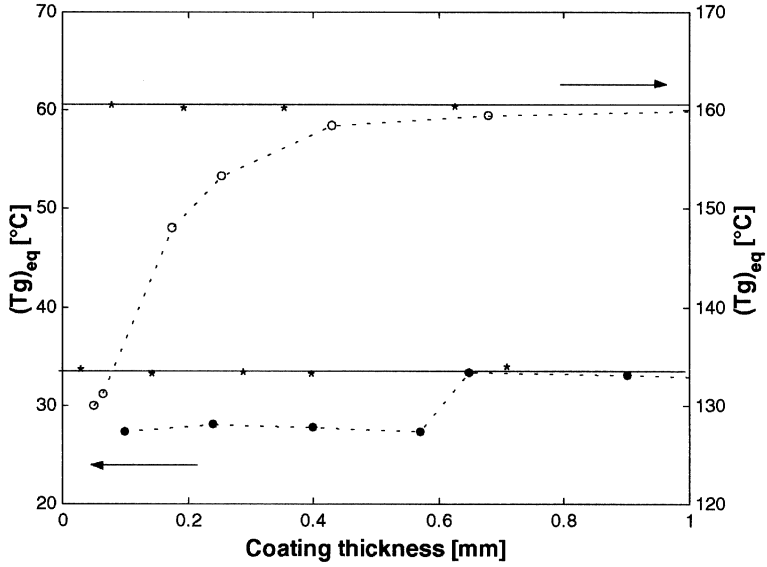

(o for IPDA, • for D400, ∗ for gold, bulk values are represented with solid line)

FIGURE 1 Variation of the equivalent glass transition temperature $(Tg)_{eq}$ as a function of the coating thickness for both DGEBA/IPDA and DGEBA/D400 systems applied on degreased titanium and gold.

than 600 μm, the equivalent glass transition temperatures were all equal to the cured bulk DGEBA-IPDA and DGEBA-D400 systems. Thus, it can be assumed that for thin coatings, a different epoxy network was formed. The interphase thickness can be defined as the region where the properties differ from the bulk. In the case of the degreased titanium substrate, the interphase thickness is around 600 μm. This means that for a 1 mm-thick coating, the first 600 μm from the substrate surface correspond to the interphase and that only the remaining outer 400 μm will have the same properties as the bulk polymer. The same phenomena has been observed for the degreased aluminum substrate, but the interphase thickness is half that of titanium [38].

Monomer Characterization

To characterize the chemical changes occurring, liquid monomers D400, IPDA, and DGEBA were placed between two degreased metallic substrates and kept at room temperature for 3 h. Then, the "modified"

liquid monomers were scraped from their metallic substrates with a PTFE spatula and visually compared with the pure monomers. All pure monomers (D400, IPDA, and DGEBA) were transparent. Modified DGEBA or D400 from aluminium- titanium- or gold-coated substrates remains transparent. The IPDA monomers from both aluminium and titanium substrates became milky white. After 2 h in test tubes separation was observed. The floating part remained transparent while the precipitate was milky white (see Figure 2). Transmittance FTIR spectra of pure DGEBA and aluminum-, titanium- or gold-modified DGEBA are identical. Also, spectra of pure IPDA, modified IPDA after application onto gold-coated substrate, and the floating part of modified IPDA on aluminum (not represented here) are identical. Then, it can be suggested that no reaction occurred between DGEBA and the metallic surfaces, neither DGEBA nor diamine monomers (IPDA and D400) reacts with gold-coated substrates, and that the floating part of modified diamine monomers mainly consist of pure diamine monomer. FTIR spectra of modified diamines after application on aluminum-, or gold-coated substrate are shown in Figures 3 and 4, respectively, IPDA and D400, and compared with the pure monomer ones. New bands (from 1100–1350 cm^{-1} and 600–700 cm^{-1}) are observed only when IPDA or D400 were applied onto aluminum (or titanium) substrates, meaning that the diamine monomer reacts with aluminium (or titanium) substrate surfaces.

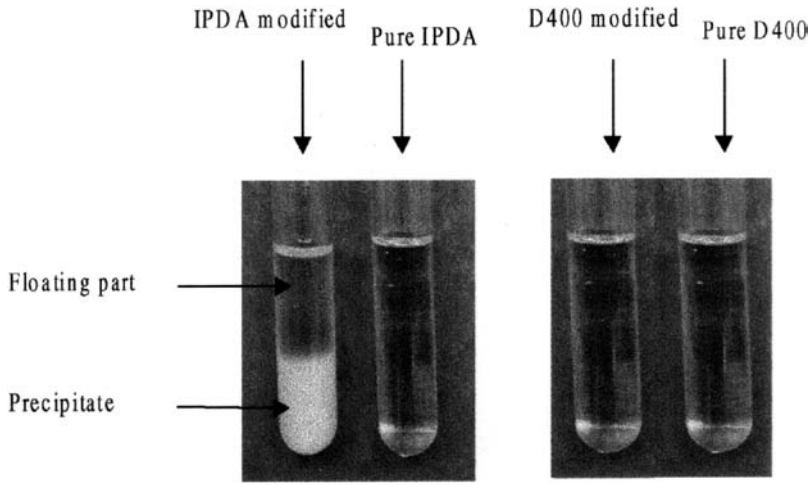

FIGURE 2 Photographs of pure IPDA or D400 and aluminium-modified IPDA or D400 after 2 h in test tube.

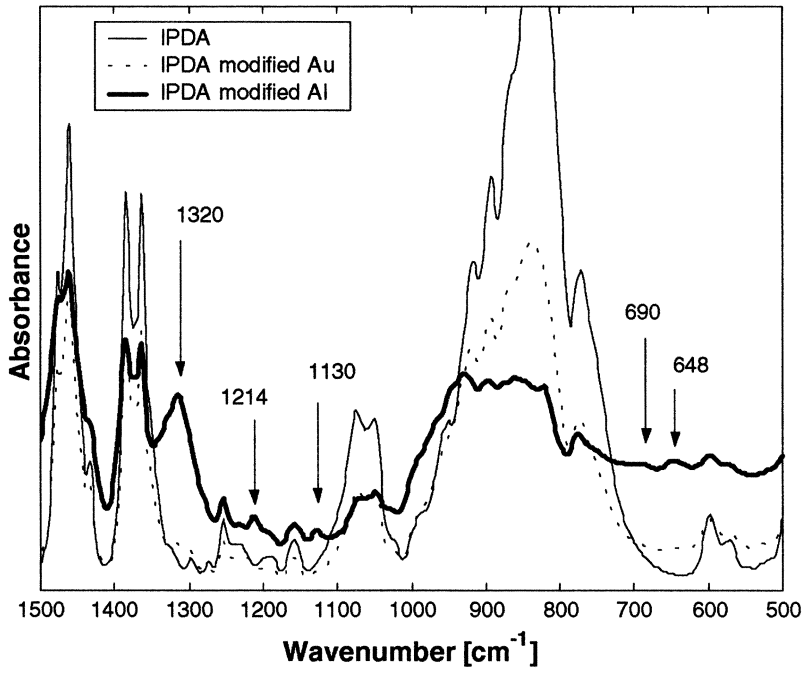

FIGURE 3 FTIR spectra of pure IPDA, Al-modified IPDA, and Au-modified IPDA.

One drop of the precipitate part of aluminum- and titanium-modified IPDA was placed between two glass plates and observed using a polarized optical microscope (Figure 5). Crystals in the modified IPDA liquid were observed. These crystals were responsible for the white milky aspect of the precipitate and express the precipitation of a newly formed species as suggested by FTIR when IPDA monomer reacted with the metallic oxide and/or hydroxide surface. No crystals have been observed in the aluminum-modified D400 after an application of 3 h. However, when the D400 is applied onto metallic substrate for 24 h, crystals were also observed as shown in Figure 6. That points out the effect of both the solubility product and the dissolution rate of the oxide-hydroxide metallic layer by basic amine monomers. In order to point out the partial dissolution of the oxide or hydroxide metallic surface by the amine, taking into account the basic nature of the pure diamine curing agent (pH = 12 for IPDA and 12.1 for D400), partial reflectance FTIR spectra (Figure 7) of IPDA applied onto sul-

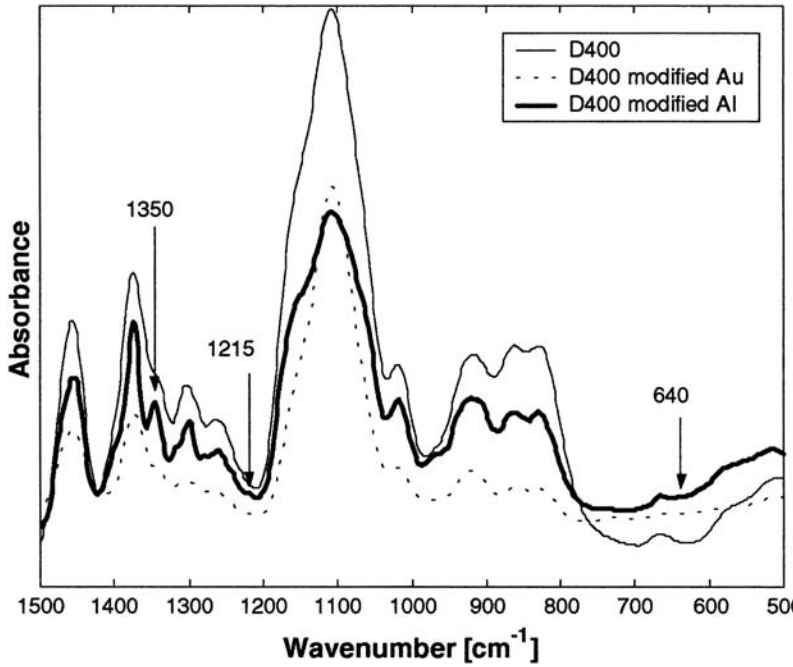

FIGURE 4 FTIR spectra of pure D400, Al-modified D400, and Au-modified D400.

furic-chromic–etched aluminum were recorded versus time and compared with the spectrum of the metallic substrate. Two broad bands were observed near 2800 and 3300 cm^{-1} corresponding to the CH, CH_2 or NH, NH_2, and OH groups, respectively. The decrease of OH band intensities demonstrates the dissolution of the metallic hydroxide layer by the monomer. Thus, the hypothesis of the dissolution of the metallic oxide and/or hydroxide by the basic diamine monomers is strengthened. When diamine monomer was mixed with epoxy prepolymer, the same phenomenon was observed, as shown in Figure 8. Following the partial dissolution of oxide or hydroxide superficial metallic layers, metallic ions may diffuse within IPDA or D400 liquid monomers. Experimentally, this was observed by ICP analysis of pure IPDA or D400 and the aluminium-modified IPDA or D400 monomer spectra (see Figure 9 with IPDA monomer). The presence of aluminium stands out clearly in the spectrum of the aluminium-modified IPDA. The same findings were observed with titanium [39]. Using a NMR analysis, recent works have shown that coordination bonds

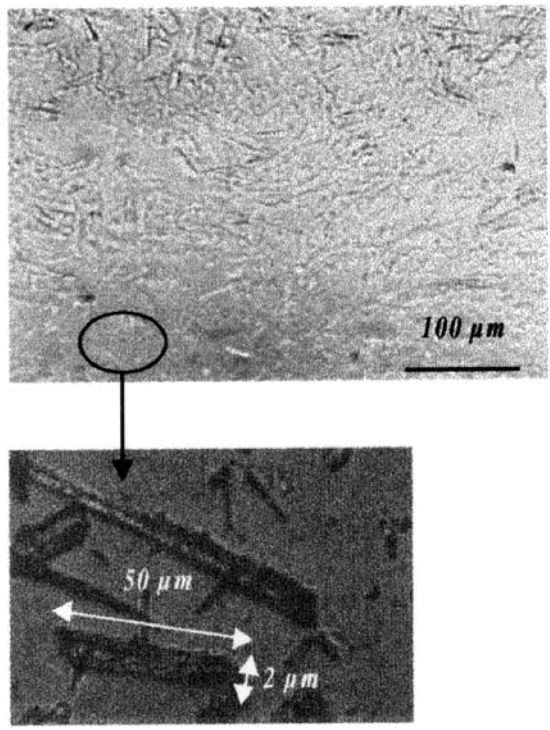

FIGURE 5 POM micrographs of the modified IPDA precipitates obtained after application on aluminium substrates for 3 h.

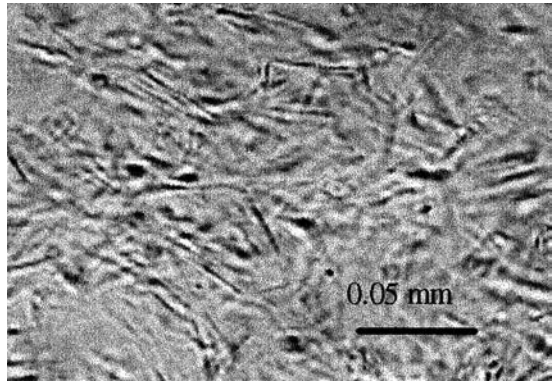

FIGURE 6 POM micrographs of the modified D400 precipitates obtained after application on aluminium substrates for 24 h.

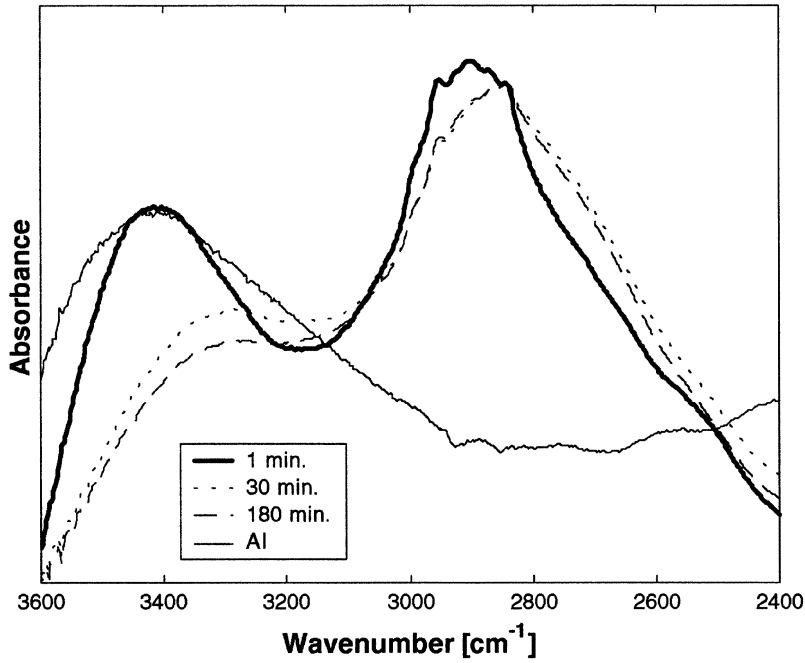

FIGURE 7 Reflectance FTIR spectra evolution when IPDA is applied on chemically etched aluminium substrate as a function of time.

between amine groups and metallic ions were formed [40]. Moreover, SEC analysis obtained from pure diamine monomer (MCDEA) and modified MCDEA with either titanium or aluminum substrates has clearly shown new small peaks twice as high as for the pure MCDEA monomer weight average molecular weight (Mw). Following chemical sorption onto the oxide or hydroxide metallic layer, the liquid diamine monomer reacts with and dissolves the metallic hydrated oxide layer to form an organo-metallic complex (or chelate) by coordination bonding between amine groups and metallic ions.

When the concentration of the organo-metallic complex is higher than its solubility limit (Ks), these complexes partially precipitate. However, when the concentration of the organo-metallic complex is lower than its solubility limit, no crystalline precipitation is expected. Then, when IPDA or D400 was applied onto metallic substrates and left for 3 h, crystals were observed only for modified IPDA monomer. However, when D400 was applied onto the metallic surface and left for at least 24 h, crystalline precipitation was observed.

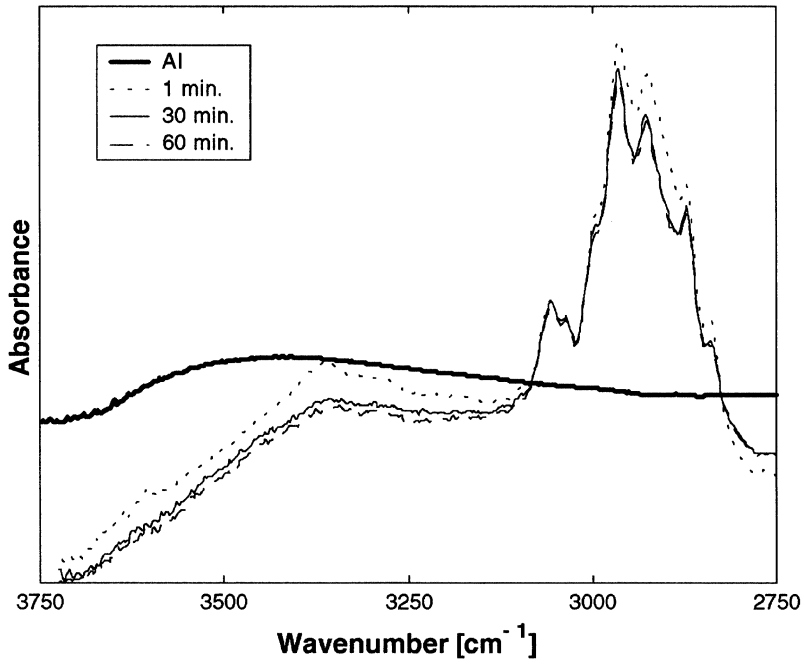

FIGURE 8 Reflectance FTIR spectra evolution when DGEBA-IPDA (a/e = 1) is applied on chemically etched aluminium substrate as a function of time.

Pure DGEBA/Modified IPDA or D400 Characterization

To understand fully the properties of interphases when DGEBA-diamine mixtures are applied onto metallic surfaces, and to verify our various hypotheses, we prepared some epoxy mixtures with pure DGEBA and aluminium-modified IPDA or D400 monomers. The stoichiometric ratio was kept equal to 1 and the curing conditions were the same as for the pure DGEBA/IPDA or D400 systems. Figure 10 contains POM photographs obtained before and after the cure cycle for pure DGEBA/aluminum-modified IPDA or D400 mixtures. Comparing Figure 5 with Figure 10, a dilution effect was observed before curing, but crystals were still present in the pure DGEBA/aluminium-modified IPDA mixtures. After curing, crystals remain observable, and all around those crystals phase separation (black parts in the photograph) can be observed. It is quite evident that the phase separation leads to the formation of a new network having a lower glass transition temperature than the initial network. This low Tg network formation can be explained by an epoxy etherification induced by the

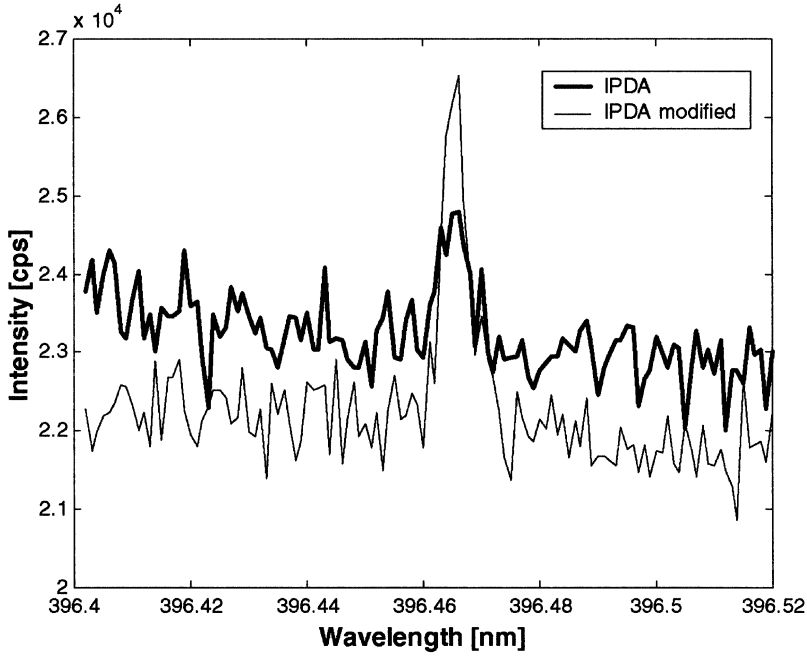

FIGURE 9 ICP analysis of pure IPDA monomer and aluminium-modified IPDA monomer.

hydroxide dissolution leading to OH^- diffusion within the liquid epoxy/aminc mixture catalyzed by the presence of metallic ions [38]. Indeed, for thin coatings on titanium or aluminum, the increase in the amount of unreacted NH or NH_2 groups [38] may be explained by the new epoxy network and the presence of crystals within the interphase region. However, for a DGEBA/aluminium-modified D400 mixtures crystals were not observed but the increase of unreacted NH or NH_2 groups was observed for thin coatings. Figure 11 describes the stoichiometric ratio variation as a function of the coating thickness for both degreased and chemically-etched aluminium according to Bouchet et al. [33]. For the thinnest coating layers, the stoichiometric ratio is close to 1.14 irrespective of the surface treatments. For this a/e ratio the corresponding Tg value is about 110°C (see Table 1). Figure 12 depicts the glass transition temperature variation of DGEBA-IPDA bulk materials and 100 μm-thick coatings on titanium alloy as a function of the stoichiometric ratio [40, 41]. Comparing Figures 11 and 12, Tg values for thin coatings cannot be associated only with the increase of the relevant a/e ratio. Moreover, Figure 13 compares the

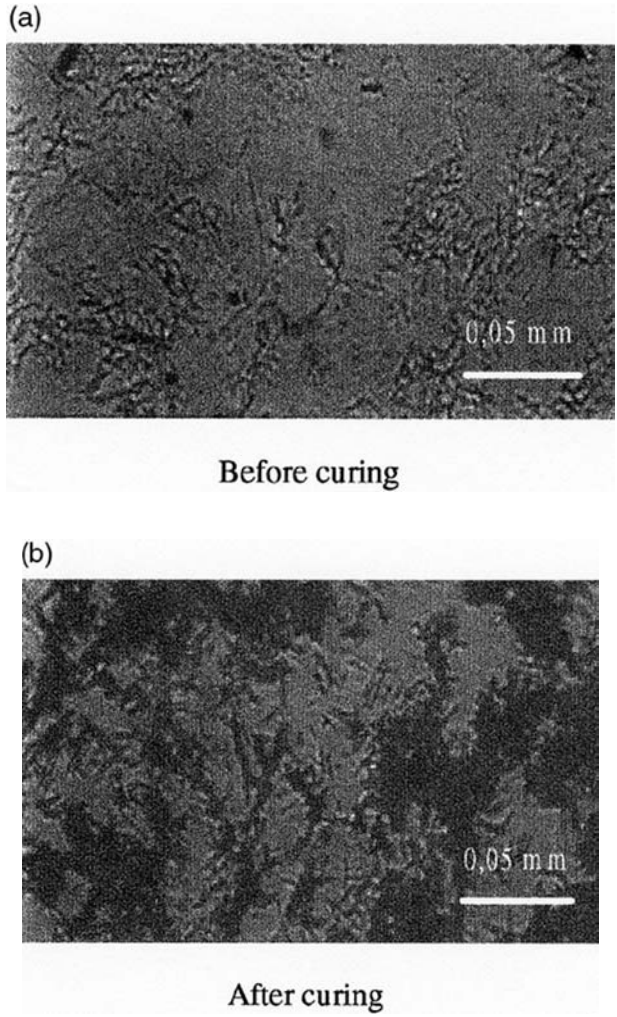

FIGURE 10 POM photographs of mixture (a/e = 1) of pure DGEBA/Al-modified IPDA.

homopolymerization ratio of bulk materials with 100 μm-thick coatings on titanium as a function of the stoichiometric ratio. Undoubtedly, the homopolymerization increases when DGEBA-IPDA mixtures were applied on titanium substrate. From Figures 5, 11, 12, and 13, we believe that the noncrystallized parts of the formed organo-metallic complexes react with the pure DGEBA monomer to form a new net-

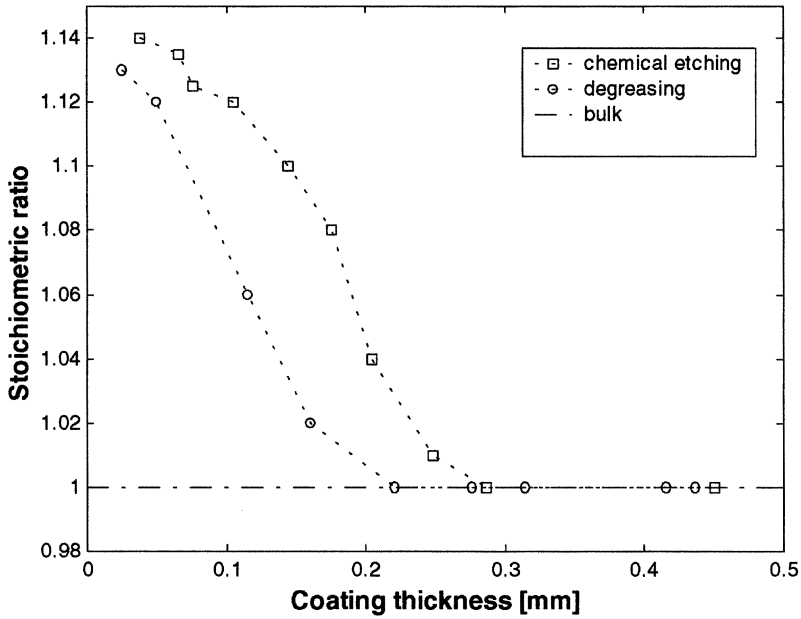

FIGURE 11 Stoichiometric ratio of the DGEBA-IPDA (a/e = 1) coating as a function of the coating thickness for both degreased and chemically etched aluminium.

work having a low Tg value. It is worth noting that studies of time-temperature-transformation (TTT) effects in the relevant networks have not been yet carried out. However, the polymerization of pure DGEBA/pure IPDA mixture (a/e = 1) either in an Al pan or a gold-coated Al pan have been studied using DSC. Respective curves

TABLE 1 Physical (Tg) and Mechanical (E) Properties of Bulk Coating and of Thin Films Applied onto Degreased Titanium and Aluminum Substrates

	Tg [°C]	E [GPa]
DGEBA/IPDA bulk	163	3.2
40 μm-thick film on Al	110	10
DGEBA/Al-modified IPDA	108	5.0
DGEBA/D400 bulk	34	1.2
46 μm-thick film on Al	26.5	1.2
DGEBA/Al-modified D400	26.8	1.2

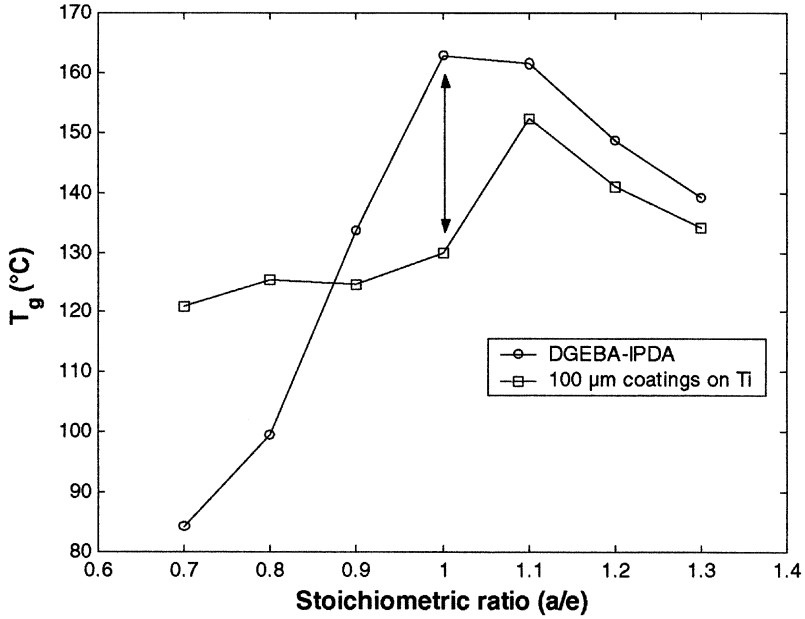

FIGURE 12 Variation of the glass transition temperature as a function of the stoichiometric ratio for DGEBA/IPDA bulk materials and 100 µm-thick coatings on titanium.

are plotted in Figure 14. Significant effects (Tg, starting point of the polymerization, the polymerization enthalpy) are definitively observed. An appropriate study will have to be considered as soon as all the relevant chemical species and functionality have been determined.

Properties of such modified bulk polymers (pure DGEBA-modified hardener) were summarized in Table 1 and were compared either with thin coatings on aluminum or to the pure bulk polymer. The properties of the pure DGEBA/aluminum-(or titanium-) modified IPDA are the same as those of thin films formed on aluminum (or titanium) substrates. This means that we have been able to reproduce within a modified bulk system the various phenomena observed for thin coatings. Moreover, it has to be noted that according to their respective liquid surface tensions, the outer part of a drop of a liquid epoxy/diamine mixture contains mainly the amine monomer, which may be considered as a surfactant [42]. Therefore, the interphase mechanisms described previously from diamine monomer applied onto metallic substrates are the same as those obtained when liquid DGEBA-diamine mixture was applied on metallic surfaces.

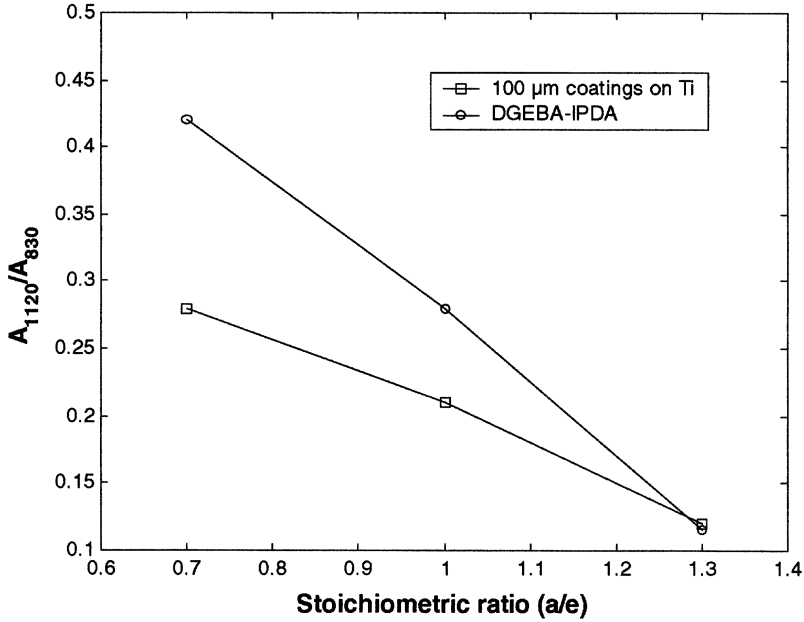

FIGURE 13 Variation of the ether/phenyl band area (A1120/A830) ratio versus the stoichiometric ratio for DGEBA/IPDA bulk materials and 100 μm-thick coatings on titanium.

Randomly dispersed, and according to their shape factor (see Figure 5), organo-metallic crystals act as short fibers in a polymer matrix [43–44] leading to an increase of 50% in the Young's modulus, as shown in Figure 15. By using a simple composite mixing rule we can point out a reinforcement due to the presence of crystals. According to Figure 10, a volume fraction of 0.35 for crystals can be assumed. Considering Young's moduli of the pure matrix (3.5 GPa) and modified material (5 GPa), the crystal modulus can be estimated to 8 GPa. It is quite evident that this value is quite reasonable for a chelate crystal. Obviously, some more work is needed to characterize the crystalline chelates fully. On the contrary, the absence of crystals in the DGEBA/aluminium-modified D400 system did not increase the Young's modulus (see Figure 15). Moreover, as shown in Figure 16, it can be observed, that the color of the bulk DGEBA/Al-modified IPDA system changes compared with the one without metal modification of the diamine monomer. This color change is due to the presence of the crystals. On the contrary, no color change is observed for the bulk

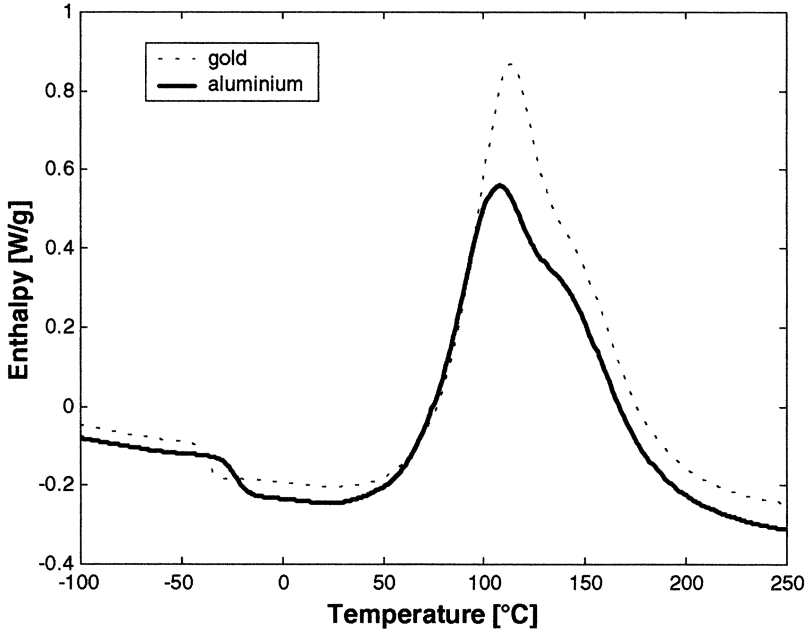

FIGURE 14 DSC thermograms of DGEBA-IPDA (a/e = 1) obtained in both gold-coated pan and Al pan.

DGEBA/Al-modified D400 system. However, this 50% increase of the Young's modulus does not explaine the huge increase (200%) in the longitudinal Young's modulus of thin films as depicted in Table 1. In a recent work [33], we have observed a drop of IPDA at the near vicinity of an aluminium substrate. Within the first hour after being deposited, it was possible to observe the crystal growth. After 3 h, a preferential orientation of crystals parallel to the surface was clearly observed. So the 10 GPa values obtained for thin coatings (see Table 1) can be explained by this preferential orientation.

Influence of Kinetics

Throughout the previous section, we have pointed out that the epoxy-metal interphase formation mechanisms result from a dissolution and a diffusion phenomenon irrespective of the metallic substrates (i.e., aluminium or titanium). This means that it is possible to control the interphase formation by limiting the contact duration between the liquid prepolymers and metallic substrates (i.e., to control the dis-

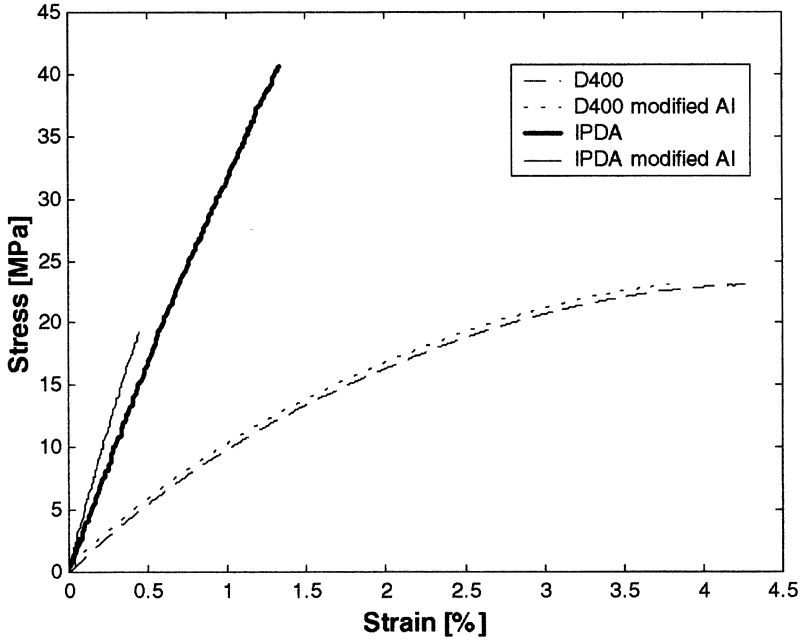

FIGURE 15 Tensile stress versus strain curves for pure DGEBA/IPDA or D400 systems and pure DGEBA/Al-modified IPDA or D400 systems.

solution rate). That can be easily achieved using an appropriate "flash" curing cycle.

Thus, to minimize the interphase, coated panels were immediately, after the application of the DGEBA-IPDA mixtures onto treated aluminium substrates (less than 5 min), introduced into an oven at 190°C and kept there for 6 h before cooling down. On the contrary, when a thick interphase is desired, liquid prepolymers are applied onto metallic substrates and kept at room temperature for 3 h before the thermal cycle (see "Monomers and Polymers" section above). In Table 2, we have reported the final physical and mechanical properties of both bulk polymers and films according to the two different curing cycles. We can observe that bulk mechanical properties (E) are identical, irrespective of the curing cycle. However, the bulk physical properties (Tg) are slightly different due certainly to diamine evaporation during the flash curing cycle. For the 30 μm-thin film on aluminium with the curing cycle (*i*), we can observe, as explained previously, that the mechanical and physical properties are quite different from the bulk ones expressing the interphase formation.

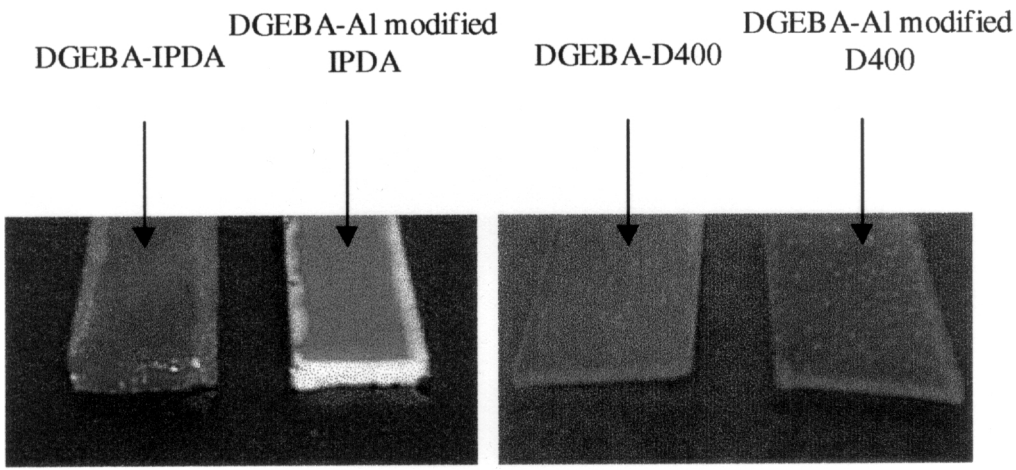

FIGURE 16 Photograph of pure DGEBA/IPDA or D400 systems and pure DGEBA/Al-modified IPDA or D400 systems after the tensile test.

TABLE 2 Mechanical (E) and Physical (Tg) Properties of DGEBA-IPDA Systems

Material	Curing cycle	E [GPa]	Tg [°C]
Bulk	**(i)**	3.2	163
	(ii)	3.1	156
30 μm-thin film on Al	**(i)**	14	110
30 μm-thin film on Al	**(ii)**	3.3	154

(i) 3 h at 20°C, 20 (60°C (2°C/min), 2 h at 60°C, 60 (140°C (2°C/min), 1 h at 140°C, 140 (190°C (2°C/min), 6 h at 190°C, cooling (8 h) in the oven to 20°C.
(ii) 6 h at 190°C, cooling (8 h) in the oven to 20°C.

However, for the 30 μm-thin film on aluminium with the flash curing cycle, mechanical and physical properties are the same as for the bulk, expressing that no interphase formation is observed or an interphase so thin is observed that we are unable to reveal it.

Practical Adhesion Measurement

The practical adhesion measurement was relevant to an adhesional failure (or within the interphase region) and, obviously, only the interphase properties have to be considered instead of the bulk ones. Recent works have reported that the consideration of the mechanical properties of the interphase are of prime importance for very thick interphases, as presented in this study, to understand the mechanical behavior of bonded structures [33, 45, 46]. To get a better understanding about the role of the interphase formation on practical adhesion, we have tested, using a three-point flexure test, two series of DGEBA-IPDA applied on treated aluminium and titanium substrates by using the two curing cycles mentioned previously (i.e., (i) and (ii)) before and after hydrothermal aging. The practical adhesion measurement results, before aging, are presented in Table 3. Let us remember that thick interphases were formed using curing cycle (i), while when using curing cycle (ii) undetected interphase formation was revealed. A practical adhesion decrease was observed as soon as the interphase was formed. According to previous works [46], we can assume that this decrease directly depends on the residual stresses created during the polymerization process. Indeed, as shown in Table 4, irrespective of the substrate's nature, the measured radius of curvature decreases when the interphase is formed. This means that the interphase formation induces an increase of residual stresses at the interphase/substrate interface. Secondly, some samples were aged in distilled water at 40°C for 24 h and kept at air-conditioned room

TABLE 3 Practical Adhesion of DGEBA-IPDA on Both Chemically Etched and Degreased Panels before Aging

With interphase formation				Without interphase formation			
Aluminium							
Degreasing		Chemical etching		Degreasing		Chemical etching	
F_{max} [N]	d_{max} [mm]	F_{max} [N]	d_{max} [mm]	F_{max} [N]	d_{max} [mm]	F_{max} [N]	d_{max} [mm]
$46.3 \pm 11\%$	$0.2 \pm 14\%$	$89.3 \pm 9\%$	$0.22 \pm 3\%$	$112 \pm 12\%$	$0.21 \pm 14\%$	$255 \pm 10\%$	$0.45 \pm 12\%$
Titanium							
Degreasing		Chemical etching		Degreasing		Chemical etching	
F_{max} [N]	d_{max} [mm]	F_{max} [N]	d_{max} [mm]	F_{max} [N]	d_{max} [mm]	F_{max} [N]	d_{max} [mm]
$17.7 \pm 10\%$	$0.12 \pm 7\%$	$28.3 \pm 8\%$	$0.32 \pm 3\%$	$68.9 \pm 12\%$	$0.48 \pm 14\%$	$110 \pm 11\%$	$0.59 \pm 13\%$

F_{max} is the ultimate load.
d_{max} is the ultimate displacement.

TABLE 4 Radius of Curvature (R_1) of DGEBA-IPDA System Applied on Metallic Substrates

Material	Curing cycle	R_1[mm]
150 μm-thin film on Al	**(i)**	$1570 \pm 10\%$
150 μm-thin film on Al	**(ii)**	$3165 \pm 15\%$
150 μm-thin film on Ti	**(i)**	$1370 \pm 8\%$
150 μm-thin film on Ti	**(ii)**	$2895 \pm 15\%$

(i) 3 h at 20°C, 20 (60°C (2°C/min), 2 h at 60°C, 60 (140°C (2°C/min), 1 h at 140°C, 140 (190°C (2°C/min), 6 h at 190°C, cooling (8 h) in the oven to 20°C.
(ii) 6 h at 190°C, cooling (8 h) in the oven to 20°C.

temperature (22 ± 2°C and $55 \pm 5\%$ R.H.) for 48 h. For all degreased panels, failures occurred during aging. Therefore, only coatings applied onto chemically etched panels were tested (Table 5). Adhesional failure was observed for all tested samples. After aging, a decrease of practical adhesion was observed for unformed interphase. On the contrary, when the interphase was formed, the practical adhesion remained quite constant. According to this result, we can assume that the interphase and, more particularly, the organometallic (chelates) complexes act as a barrier material or water diffusion (corrosion) inhibitor within the interphase region as has been reported previously [47].

TABLE 5 Practical Adhesion of Chemically Etched Panels after Aging

With interphase formation		Without interphase formation	
Aluminium			
Chemical etching		Chemical etching	
F_{max} [N]	d_{max} [mm]	F_{max} [N]	d_{max} [mm]
$135.1 \pm 7\%$	$0.27 \pm 9\%$	$116 \pm 4\%$	$0.23 \pm 5\%$
Titanium			
Chemical etching		Chemical etching	
F_{max} [N]	d_{max} [mm]	F_{max} [N]	d_{max} [mm]
$34.5 \pm 10\%$	$0.28 \pm 9\%$	$56 \pm 14\%$	$0.33 \pm 12\%$

F_{max} is the ultimate load.
d_{max} is the ultimate displacement.

CONCLUSION

When epoxy-diamine prepolymers were applied to metallic substrates, interphases between the part of the coating having the bulk properties and the metallic surface were created. Chemical, physical, and mechanical properties of the interphase formed depend on both the substrate and the nature of the diamine hardener. Using an appropriate curing cycle for prepolymers allowed us to reach both the maximum conversion of the polymer and the full interphase formation. This enabled us to suggest mechanisms of interphase formation, leading to a better understanding of its chemical, physical, and mechanical properties. When the pure DGEBA monomer was applied to the metallic surfaces or when pure diamine monomers were applied on gold-coated substrates, no chemical reaction was observed. On the contrary, when pure diamine monomers were applied on either titanium or aluminum metallic surfaces, chemical reactions occurred. Following the amine chemical sorption onto oxided or hydroxylated metallic surfaces, a partial dissolution of the surface oxide and/or hydroxide on the metallic substrate was observed according to the basic behavior of diamine monomers. Then, metallic ions diffuse within the liquid monomer mixture (epoxy-diamine) and react by coordination with the amine groups of the diamine monomers to form organo-metallic complexes (or chelates). When the concentration of the complex is higher than its solubility limit, complexes (or chelates) crystallized as sharp needles. During the curing cycle, crystals are not fully dissolved and a phase separation occurs, inducing the formation of a new epoxy network (having a low Tg) with the unprecipitated complexes. The same phenomena were observed for all kinds of metallic substrates as soon as they were covered by an oxide or hydroxide layer as shown in Figure 17 for several metallic substrates widely used in many industrial applications. In Table 6, we have reported the physical properties of such modified systems. Since dissolution and diffusion phenomena were expected, the interphase formation should be related to the liquid-solid contact duration between liquid prepolymers and metallic substrates. It was also observed that the interphase formation decreases the practical adhesion by increasing residual stresses, but the interphase formation increases the hydrothermal durability of coated samples. Indeed, results show the prime importance of the duration of the contact of liquid prepolymer systems with metallic substrates. For identical systems, overall properties of coatings, including those of the interphase, depend on the duration of contact between metallic surfaces and liquid pre-

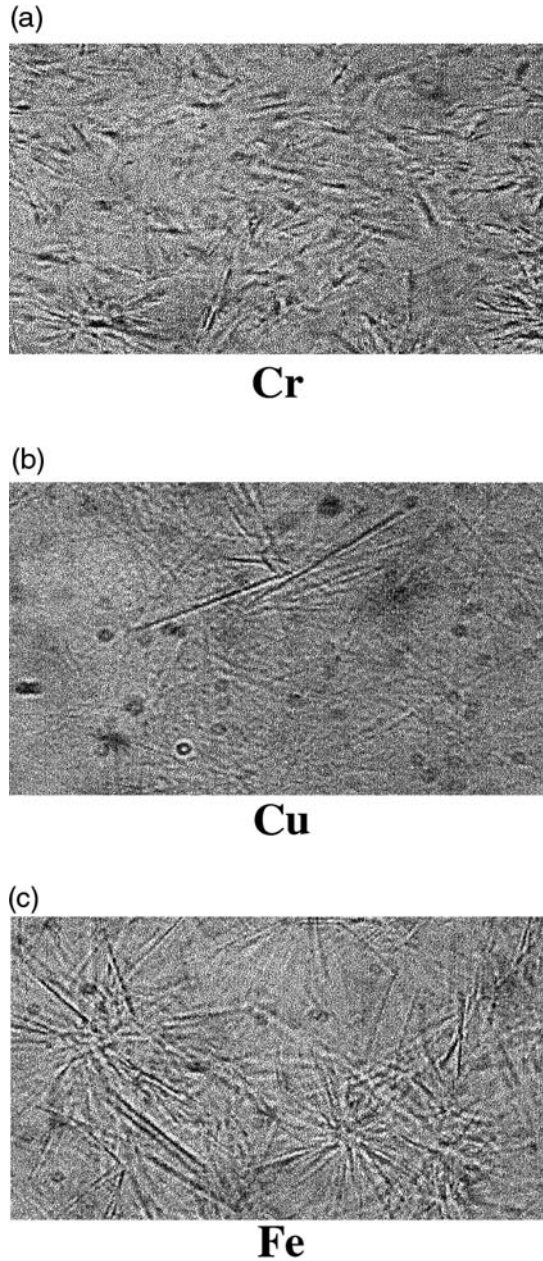

FIGURE 17 POM micrographs of the modified IPDA precipitates obtained after application on several metallic substrates. (*Continued*)

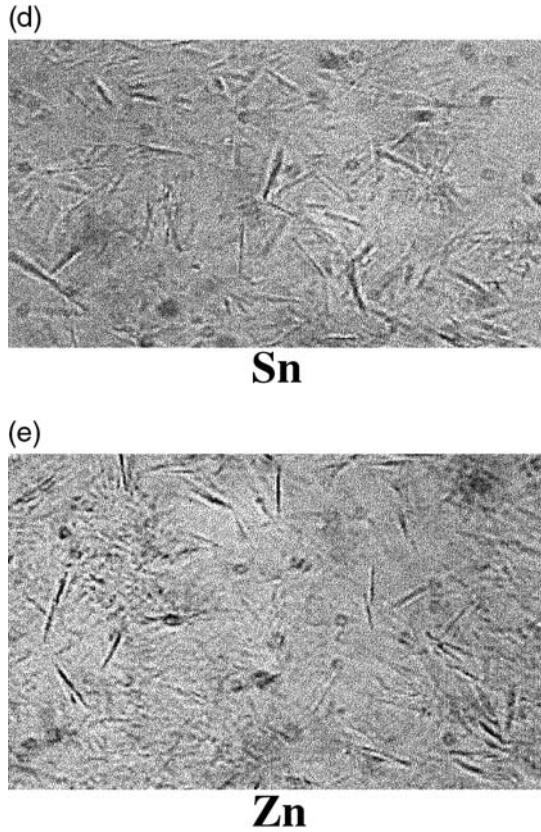

FIGURE 17 (*Continued*)

TABLE 6 Glass Transition Temperature of Pure DGEBA/IPDA Bulk and DGEBA/Modified IPDA Systems

System	Tg [°C]
DGEBA/IPDA bulk	**164**
DGEBA/**Au** modified IPDA	163
DGEBA/**Al** modified IPDA	110
DGEBA/**Ti** modified IPDA	128
DGEBA/**Cr** modified IPDA	126
DGEBA/**Zn** modified IPDA	116
DGEBA/**Sn** modified IPDA	137
DGEBA/**Fe** modified IPDA	139
DGEBA/**Cu** modified IPDA	117

polymers and can explain the different findings observed in the literature.

REFERENCES

[1] Peillex, E., *Ph.D. thesis*, Université de Lyon 1, France, 1996.
[2] Fauquet, C., *Ph.D. thesis*, Université Paris 6, France, 1992.
[3] Walker, P., *J. Coating Technol.* **52**, 49–56 (1980).
[4] Guminski, R. D. and Meredith, F. M. P., *J. Oil. Colour Chem. Assoc.* **44**, 93–98 (1961).
[5] Hine, P. J., Muddarris, S. E. L. and Packham, D. E. *J. Adhesion Sci. Technol.* **1**, 69–78 (1987).
[6] De'neve, B., *Ph.D. thesis*, Ecole Nationale Supérieure des Mines de Paris, France, 1993.
[7] Dillingham, R. G. and Boerio F. J., *J. Adhesion* **24**, 315–335 (1987).
[8] Nigro, J. and Ishida, H., *J. Appl. Polym. Sci.* **38**, 2191–2204 (1989).
[9] Gaillard, F., Hocquaux, H., Romand, M. and Verchère, D., *Proceedings of Euradh'92* (Karlsruhe, Germany, 1992), pp. 122–127.
[10] Verchère, D., Hocquaux, H., Marquais, T. and Gaillard, F., *Proceedings of Euradh'92* (Karlsruhe, Germany, 1992), pp. 488–495.
[11] De Vries, J. E., Haack, L. P., Holubka, J. W. and Dickie, R. A., *J. Adhesion. Sci. Technol.* **3**, 203–211 (1989).
[12] Hong, S. G., Cave, N. G. and Boerio, F. J., *J. Adhesion* **36**, 265–279 (1992).
[13] Holubka, J. W. and Ball, J. C., *Ind. Eng. Chem. Res.* **28**, 48–51 (1989).
[14] Kollek, H., *Int. J. Adhesion Adhesives* **5**, 75–80 (1985).
[15] March, J., Minel, L., Barthes-Labrousse, M. G. and Gorse, D., *Appl. Surface Sci.* **133**, 270–286 (1998).
[16] Crompton, G. S., *J. Mater. Sci.* **24**, 1575–1581 (1989).
[17] Kim, Y. H., Walker, G. F., Kim, J. and Park, J., *J. Adhesion Sci. Technol.* **1**(4) 331–339 (1987).
[18] Allara, D. I. and White, C. W., *Amer. Chem. Soc.* 273–284 (1978).
[19] Entenberg, A., Lindberg, V., Fendrock, L., Hong, S.-K., Chen, T. S. and Horwath, R. S., In: *Metallized Plastics 1: Fundamental and Applied Aspects*, K. L. Mittal and J. R. Susko, Eds. (Plenum Press, New York, 1989), pp. 103–113.
[20] Von Preissing, F. J., *J. Appl. Phys.* **66**, 4262–4628 (1989).
[21] Scafidi, P. and Ignat, M., *J. Adhesion Sci. Technol.* **12**, 1219–1242 (1998).
[22] Orsini, H. and Schmit, F., *J. Adhesion* **43**, 55–68 (1993).
[23] Thouless, M. D. and Jensen, H. M., *J. Adhesion Sci. Techn.* **8**, 579–586 (1994).
[24] Mulville, D. R. and Vaishnav, R. N., *J. Adhesion* **7**, 215 (1975).
[25] Mittal, K. L., In: *Adhesion Measurement of Thin Films, Thick Films and Bulk Coatings*, K. L. Mittal, Ed. (ASTM, Philadelphia, 1978), pp. 5–17.
[26] Sharpe, L. H., *J. Adhesion* **4**, 51 (1972).
[27] Safavi-Ardebili, V., Sinclair, A. N. and Spelt, J. K., *J. Adhesion* **62**, 93–111 (1997).
[28] Finlayson, M. F. and Shah, B. A., *J. Adhesion Sci. Technol.* **4**, 431–441 (1990).
[29] Bouchet, J., Roche, A. A. and Hamelin, P., *Thin Solid Films* **355–356**, 270–276 (1999).
[30] Sindt, O., Perez, J. and Gerard, J. F., *Polymer* **37**, 2989–2998 (1995).
[31] Bonnaud, L., *Ph.D. thesis*, INSA de Lyon, France, 1999.
[32] Masood Siddiqi, H., *Ph.D. thesis*, INSA de Lyon, France, 1997.

[33] Bouchet, J., Roche, A. A. and Jacquelin, E., *J. Adhesion Sci. Technol.* **15**, 321–343 (2001).
[34] Roche, A. A., *Ph.D. thesis*, Université de Lyon 1, France, 1983.
[35] Roche, A. A., Dumas, J., Quinson, J. F. and Romand, M., In: *Mechanics and Mechanisms of Damage in Composites and Multi-materials*, D. Baptiste, Ed. (Mechanical Engineering Publications, London, 1991), pp. 269–276.
[36] Ripling, E. J., Santner, J. S. and Crosley, P. B., In: *Adhesive Joints: Formation, Characteristics, and Testing*, K. L. Mittal, Ed. (Plenum Press, New York, 1984), pp. 755–788.
[37] Roche, A. A., Dole, P. and Bouzziri, M., *J. Adhesion Sci. Technol.* **8**, 587–609 (1994).
[38] Bentadjine, S., Roche, A. A. and Bouchet, J., In: *Adhesion Aspects of Thin Films*, Volume I, K. L. Mittal, Ed. (VSP, Utrecht, The Netherlands, 2001), pp. 239–260.
[39] Roche, A. A., Bouchet, J. and Bentadjine, S., *Int. J. Adhesion and Adhesives*, 2002, (in press).
[40] Bentadjine, S., Roche, A. A., Massardier, V. and Petiaud, R., *Polymer* **42**, 6271–6282 (2001).
[41] Bentadjine, S., *Ph.D. thesis*, INSA de Lyon, France, 2000.
[42] Dong, C., Pascault, J. P. and Sage, D., *Makromol. Chem.* **192**, 867–882 (1991).
[43] Saadi, A. R. and Piggot, M. R., *J. Mater. Sci.* **20**, 413–437 (1985).
[44] Mehan, M. L. and Schadler, L. S., *Composites Sci. Technol.* **60**, 1013–1026 (2000).
[45] Bouchet, J., Roche, A. A., Jacquelin, E. and Scherer, G. W., In: *Adhesion Aspects of Thin Films*, Volume I, K. L. Mittal, Ed., (VSP, Utrecht, The Netherlands, 2001).
[46] Bouchet, J., Roche, A. A. and Jacquelin, E., *J. Adhesion Sci. Technol.* **15**, 345–369 (2001).
[47] Duprat, M. and Dabozi, F., *Corrosion* **37**, 89–92 (1981).